IHJPAS. 36 (4) 2023

Ibn Al-Haitham Journal for Pure and Applied Sciences
Journal homepage: jih.uobaghdad.edu.iq

# Novel Approximate Solutions for Nonlinear Initial and Boundary Value Problems

**Othman Mahdi Salih***
Department of Mathematics, College of Education for Pure Sciences Ibn AL-Haitham, University of Baghdad, Baghdad, Iraq.

**Majeed A. AL-Jawary**
Department of Mathematics, College of Education for Pure Sciences Ibn AL-Haitham, University of Baghdad, Baghdad, Iraq.

**Mustafa Turkyilmazoglu**
-Department of Mathematics, Hacettepe University, Ankara, Turkey.
-Department of Medical Research, China Medical University Hospital, China Medical University, Taichung, Taiwan.

***Corresponding Author:** othman.m.s@ihcoedu.uobaghdad.edu.iq

**Article history: Received 03 Februray 2022, Accepted 14 March 2023, Published in October 2023**

**doi.org/10.30526/36.4.3265**

**Abctract**

This paper investigates an Effective Computational Method (ECM) based on the standard polynomials used to solve some nonlinear initial and boundary value problems in engineering and applied sciences. Moreover, the effective computational methods in this paper were improved by suitable orthogonal base functions, especially the Chebyshev, Bernoulli, and Laguerre polynomials, to obtain novel approximate solutions for some nonlinear problems. These base functions enable the nonlinear problem to be effectively converted into a nonlinear algebraic system of equations, which are then solved using Mathematica®12. The Improved Effective Computational Methods (I-ECMs) have been implemented to solve three applications involving nonlinear initial and boundary value problems: the Darcy-Brinkman-Forchheimer equation, the Blasius equation, and the Falkner-Skan equation, and a comparison between the proposed methods has been presented. Furthermore, the Maximum Error Remainder ($MER_n$) has been computed to prove the proposed methods' accuracy. The results convincingly prove that ECM and I-ECMs are effective and accurate in obtaining novel approximate solutions to the problems.

**Keywords:** Darcy-Brinkman-Forchheimer equation; Blasius equation; Falkner-Skan equation; Chebyshev polynomials; Bernoulli polynomials; Laguerre polynomials.

## 1. Introduction

There are many problems in engineering and applied sciences, such as fluid flow models, mechanical engineering, and mathematical physics, which can be described by nonlinear ordinary differential equations [1]. This leads to significant computational difficulties for nonlinear boundary conditions, particularly for nonlinear initial value problems [2]. Since the exact solutions to these problems are often complicated or occasionally may not be available. Therefore, there is a great need to develop efficient, novel approximate, and numerical methods to solve these problems [3 and 4].

Numerous analytical and approximate methods for solving nonlinear differential equations have been introduced and developed by authors around the world, such as the advanced Adomian decomposition method [5], the Variational Iteration Method (VIM), the Differential Transformation Method (DTM) [6], the finite difference methods [7], the optimal quartic B-spline collocation method [8], the homotopy analysis method with Padé approximations [9], the Chebyshev operational matrix method [10], the Bernoulli matrix method [11], the Laguerre collocation method [12]. In particular, AL-Jawary et al. [13] have applied the Daftardar-Jafari Method (DJM), the Temimi-Ansari Method (TAM), and the Banach Contraction Method (BCM) to obtain the solution for the Jeffery-Hamel flow problem. Agom et al. [14] have implemented the Homotopy Perturbation Method (HPM) and the Adomian Decomposition Method (ADM) for solving the $12^{th}$-order boundary value problems in finite domains. Also, Singh [15] used the modified homotopy perturbation approach to solve a set of nonlinear Lane-Emden equations.

Ibraheem et al. [16] have recently implemented the operational matrix of Legendre polynomials to solve nonlinear thin-film flow problems. Gürbüz et al. [17] used the matrix relations between the Laguerre polynomials and their derivatives to study second-order nonlinear ordinary differential equations with quadratic and cubic terms and several other approximation methods for instance, see [18-23].

In recent years, approximation methods for analyzing linear systems of ordinary differential equations using orthogonal series have been widely developed. These are known as spectral methods, assuming that a truncated orthogonal series expansion can reasonably approximate the solution. Depending on the nature of the problem, a variety of orthogonal series have been used, such as the Walsh series, block-pulse, Laguerre, Chebyshev, Fourier series, and others [24].

Furthermore, orthogonal functions and polynomial series have attracted significant attention because they have been instrumental in treating various dynamical system problems. The main feature of this technique is that it reduces these problems to the solution of a system of algebraic equations by using the method of operational matrices based on orthogonal polynomials [25], such as Chebyshev polynomials [26], Bernoulli polynomials [27], and Laguerre polynomials [28], which significantly simplifies the problems and allows them to be solved by any computational program.

More recently, Turkyilmazoglu [29] has proposed and used an analytical approximation method, namely the ECM, to solve various types of problems, such as nonlinear Lane-Emden-Fowler equations [29], Fredholm integro-differential equations [30], Volterra-Fredholm-Hammerstein integro-differential equations [31], heat transfer of fin problems [32], and initial and boundary value problems with difficult exact solutions [33]. Moreover, the approach depends on appropriate base functions, such as the standard polynomials. In addition, the solution of the nonlinear equations is transformed into a nonlinear algebraic system with unknown standard polynomial coefficients, which can be solved numerically or analytically with modern software.

The current paper aims to use the ECM based on the standard polynomials to solve three applications involving nonlinear initial and boundary value problems: the Darcy-Brinkman-Forchheimer equation, the Blasius equation, and the Falkner-Skan equation, which are found in engineering and applied sciences. The main goals are to develop the ECM by introducing various orthogonal polynomials, such as Chebyshev, Bernoulli, and Laguerre polynomials, and to form a novel collection of the I-ECMs. The final goal is to implement the I-ECMs to solve these problems.

The paper is organized as follows: Section two presents the mathematical formulations of three nonlinear models. Section three introduces the basic concepts of the proposed methods. Section four displays the implementation of the ECM and I-ECMs to solve three nonlinear problems and discusses the results. Finally, section five presents the conclusions.

## 2. The Mathematical Formulations of Nonlinear Models

### 2.1 The Darcy-Brinkman-Forchheimer Equation

Consider the following steady-state, pressure-driven, fully developed parallel flow over a horizontal channel filled with a porous medium [34], as demonstrated in Figure 1:

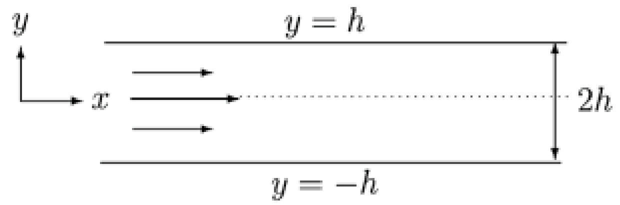


**Figure 1.** Parallel flow in a fluid-saturated porous channel [35].

The positions of the bottom and top plates are $y = h$ and $y = -h$, respectively. The velocity takes the form $u = (y(x), 0, 0)$ and the flow is in the $x$-axis direction. The Darcy-Brinkman-Forchheimer equation, which has the following form [36], is known to determine the flow in the channel.

$$y''(x) - s^2\, y(x) - F\, s\, y^2(x) + \frac{1}{M} = 0, \qquad (1)$$

subjected to the boundary conditions:

$$y'(0) = 0, \qquad y(1) = 0. \qquad (2)$$

where $F$ stands for the Forchheimer number, $s$ for the shape parameter of the porous medium, and $M$ for the viscosity ratio.

The Darcy-Brinkman-Forchheimer equation has been solved analytically and approximately using a variety of methods, such as the homotopy analysis method [37], the finite difference method [38], the optimal asymptotic Galerkin homotopy method [36], and the Tau homotopy analysis method [34]. In particular, Adewumi et al. [39] obtained the approximate solutions for the model by using the hybrid method in combination with the Chebyshev collocation method with Laplace and differential transform methods. Motsa et al. [35] implemented the spectral homotopy analysis approach to obtain an accurate result for the model. In addition, Abbasbandy et al. [40] obtained a closed-form solution of forced convection in a porous saturated channel.

## 2.2 The Blasius Equation

The Blasius equation is the well-known third-order nonlinear ordinary differential equation that appeared in several boundary layer problems involving a fluid's two-dimensional laminar viscous flow through a flat plate. The following equation presents it as a governing equation for fluid dynamics [41]:

$$y'''(x) + \frac{1}{2} y(x)\, y''(x) = 0, \tag{3}$$

subjected to the boundary conditions:

$$y(0) = 0,\;\; y'(0) = 0,\;\; y'(\infty) = 1. \tag{4}$$

The second derivative of $y(x)$ at zero is important in the Blasius equation to evaluate the shear stress on the plate. Numerous authors have tried to solve this problem and obtained various numbers for this value. For more details, see [42-44]. Therefore, the boundary conditions of the Blasius equation become:

$$y(0) = 0,\;\; y'(0) = 0,\;\; y''(0) = \alpha. \tag{5}$$

The value of $\alpha = 0.3320573$ will be utilized in the present work, as stated in [43].

Several numerical and analytical techniques have been used to solve the Blasius equation, such as the homotopy analysis method [45], the optimal homotopy asymptotic method [46], the variational iteration method [47], and the Adomian decomposition method [48]. In addition, Khataybeh et al. [42] applied the classical operational matrices of the Bernstein polynomial to solve the equation. Also, Parand and Taghavi [49] implemented a collocation method based on a rationally scaled generalized Laguerre function to solve the Blasius equation.

## 2.3 The Falkner-Skan Equation

The boundary layer equations are a significant class of nonlinear ordinary differential equations with several uses in fluid dynamics and physics [50]. One of these equations is the stationary Falkner-Skan boundary layer equation. The Falkner-Skan equation was initially put out by Falkner and Skan in 1931[51]. This equation is essential for numerous applications, including fluid mechanics, aerospace, heat transfer, glass applications, and polymer investigations [20].

The third-order ordinary differential equation of the Falkner-Skan equation over a semi-infinite domain is given by [52]:

$$y'''(x) + k y(x)\, y''(x) + \beta\, [\epsilon^2 - (y'(x))^2] = 0, \tag{6}$$

subjected to the boundary conditions:

$$y(0) = 0,\;\; y'(0) = 1 - \epsilon,\;\; y'(\infty) = \epsilon, \tag{7}$$

where $k = 1$ is constant.

The velocity ratio parameter is denoted by $\epsilon$, and the pressure gradient parameter by $\beta$. The Equation (6) is known as the Blasius equation when $\beta = 0$ and $k = \frac{1}{2}$, the Homann flow issue when $\beta = \frac{1}{2}$ and $k = 1$, and the Hiemenz flow problem when $\beta = 1$ and $k = 1$, see [20].

The initial condition $y''(0) = -0.832666$ has been derived by the authors from the boundary condition $y'(\infty) = \epsilon$, using the Padé approximation method [53], and this value will be utilized in the current paper. As a result, the following are the initial conditions for the Falkner-Skan equation:

$$y(0) = 0,\;\; y'(0) = 1 - \epsilon,\;\; y''(0) = -0.832666. \tag{8}$$

The Falkner-Skan equation has been solved by using a variety of techniques, like the homotopy perturbation method [54], the homotopy analysis method [55], the Adomian decomposition method [56], the differential transformation method [57], the iterative transformation method [58], the Legendre rational polynomials method [59], the shifted Chebyshev collocation method [60], and the modified rational Bernoulli functions [61].

## 3. The Basic Concepts of the Proposed Methods

The fundamental ideas of the suggested methods are presented in this section. In addition, the orthogonal polynomials and operational matrices will be introduced as instruments for improving the ECM approach to obtain novel approximate solutions to specific nonlinear initial and boundary value problems described in section two.

### 3.1 The Basic Concepts of the ECM and Their Operational Matrices

Consider the following $n^{th}$- order ordinary differential equation [29]:

$$G\left(x, y, y', y'', \dots, y^{(n)}\right) = f(x), \qquad a \le x \le b, \tag{9}$$

subjected to the initial condition: $y^{(k)}(a) = \mu_k, \quad 0 \le k \le n-1,$ (10)

or with the boundary conditions: $y^{(k)}(a) = \omega_k, \ \ y^{(k)}(b) = \gamma_k, \quad 0 \le k \le \frac{n}{2} - 1.$ (11)

Where $\mu_k$, $\omega_k$, and $\gamma_k$ are constants and $f(x)$ is a known function.

The essential assumption is that the Equation (9) has a unique solution when the initial or boundary conditions are determined in the Equations (10) or (11). Moreover, a linear combination of $n^{th}$-order functional series based on standard polynomials may be used to represent the unknown function $y(x)$ as follows:

$$y(x) = \sum_{k=0}^{n} a_k \, \psi_k(x) = \boldsymbol{\Psi}(x) \, \boldsymbol{A}, \tag{12}$$

where $\boldsymbol{\Psi}(x) = [1 \ \ x \ \ x^2 \ x^3 \ \dots \ x^n]$ and $\boldsymbol{A} = [a_0 \ a_1 \ a_2 \dots a_n]^T$, such that $a_k, k = 0, \dots, n,$ are the coefficients, whose values will be specified later.

Assume $\boldsymbol{\Psi}(x)$ has the following derivatives:

$$\boldsymbol{\Psi}'(x) = \boldsymbol{\Psi}(x) \, \boldsymbol{B}^* \, , \boldsymbol{\Psi}''(x) = \boldsymbol{\Psi}(x) \, (\boldsymbol{B}^*)^2, \dots \, , \boldsymbol{\Psi}^{(n)}(x) = \boldsymbol{\Psi}(x) \, (\boldsymbol{B}^*)^n,$$

where $\boldsymbol{B}^*{}_{(n+1)\times(n+1),}$ is the operational matrix and its entry values are from the following in the standard polynomials:

$$\boldsymbol{B}^* = \begin{bmatrix} 0 & 1 & 0 & & 0 \\ 0 & 0 & 2 & \cdots & 0 \\ 0 & 0 & 0 & & 0 \\ & \vdots & & \ddots & \vdots \\ 0 & 0 & 0 & & n \\ 0 & 0 & 0 & \cdots & 0 \end{bmatrix}_{(n+1)\times(n+1)}$$

Thus, the forms presented below can be used to define the derivatives of the function $y(x)$:

$$y^{(n)}(x) = \boldsymbol{\Psi}(x) \, (\boldsymbol{B}^*)^n \, \boldsymbol{A}, \qquad \text{where, } \ n \ge 1. \tag{13}$$

Then, the Equations (12) and (13) are substituted into the Equations (9), (10), and (11), to provide the following result:

$$G(x, \ \boldsymbol{\Psi}(x) \, \boldsymbol{A}, \ \boldsymbol{\Psi}(x) \, \boldsymbol{B}^* \, \boldsymbol{A}, \ \boldsymbol{\Psi}(x) \, (\boldsymbol{B}^*)^2 \, \boldsymbol{A}, \dots, \boldsymbol{\Psi}(x) \, (\boldsymbol{B}^*)^n \, \boldsymbol{A}) = f(x), \tag{14}$$

with, $\boldsymbol{\Psi}(a) \, (\boldsymbol{B}^*)^k \, \boldsymbol{A} = \mu_k \, , \quad 0 \le k \le n-1,$ (15)

and, $\boldsymbol{\Psi}(a) \, (\boldsymbol{B}^*)^k \, \boldsymbol{A} = \omega_k, \quad \boldsymbol{\Psi}(b) \, (\boldsymbol{B}^*)^k \, \boldsymbol{A} = \gamma_k, \quad 0 \le k \le \frac{n}{2} - 1.$ (16)

Moreover, the inner product in the Hilbert space $H = L^2[0,1]$, is defined as follows:

$$\langle g_1, g_2 \rangle = \int_0^1 g_1(x)\, g_2(x)\, dx. \tag{17}$$

Also, the set of functions $\boldsymbol{\Omega} = \{\Omega_0, \Omega_1 \dots, \Omega_k\}$, are linearly independent in $H$, where $\Omega_k = x^k, 0 \le k \le n$, is the base function of the standard polynomials [29].

Therefore, applying the inner product of the set of base functions $\boldsymbol{\Omega}$ with the left and right sides of the Equation (14), as given in the Equation (17), yields the matrix equation shown below [31]:

$$\boldsymbol{F} = \boldsymbol{G}, \tag{18}$$

where the $i^{th}$ row of $\boldsymbol{F}$ and $\boldsymbol{G}$ in the matrix equation given in the Equation (18) includes the following:

$$\langle \Omega_i, G(x,\ \boldsymbol{\Psi}(x)\,\boldsymbol{A},\ \boldsymbol{\Psi}(x)\,\boldsymbol{B}^*\,\boldsymbol{A},\ \boldsymbol{\Psi}(x)\,(\boldsymbol{B}^*)^2\,\boldsymbol{A}, \dots, \boldsymbol{\Psi}(x)\,(\boldsymbol{B}^*)^n\,\boldsymbol{A})\ \rangle,\ \langle \Omega_i, f(x) \rangle,\ \ 0 \le i \le n. \tag{19}$$

Finally, some of the entries in the matrix equation (Equation(18)) will be modified when the initial or boundary conditions from the Equations (15) and (16) are substituted. As a result, a system of $(n + 1)$ non-linear algebraic equations are produced, with unknown coefficients $\boldsymbol{A}$. Then, solve these algebraic equations numerically with applicable programs or sometimes analytically. Unique values for the unknown coefficients $\boldsymbol{A} = [a_0\ a_1\ a_2 \dots a_n]$ can be acquired, which are substituted into the Equation (12) to obtain the approximate solution of the Equation (9).

### 3.2 The Chebyshev Polynomials and Their Operational Matrices

The following is the definition of the first kind of the Chebyshev polynomials $\boldsymbol{T}_n(x)$ of degree $n$:

$$\boldsymbol{T}_n(x) = \sum_{k=0}^{n} (-1)^{n-k}\, 2^k \frac{(n+k-1)!}{(n-k)!\,(2k)!}(x+1)^k. \tag{20}$$

The function $y(x)$ can be represented by the $(n+1)$-terms of the Chebyshev polynomials of the first kind as below [10]:

$$y(x) = \sum_{k=0}^{n} a_k\, \boldsymbol{T}_k(x) = \boldsymbol{A}^T\, \boldsymbol{\Psi}(x), \tag{21}$$

where, $\boldsymbol{\Psi}(x) = [\boldsymbol{T}_0(x), \boldsymbol{T}_1(x), \boldsymbol{T}_2(x), \dots, \boldsymbol{T}_n(x)]^T$ and $\boldsymbol{A} = [a_0\ a_1\ a_2 \dots a_n]^T$, such that $a_k, k = 0, \dots, n$, are the unknown Chebyshev polynomials coefficients of the first kind, whose values will be determined later.

Moreover, the derivatives of $\boldsymbol{\Psi}(x)$ can be regarded as:

$$\boldsymbol{\Psi}'(x) = \boldsymbol{B}_{\boldsymbol{T}}^*\, \boldsymbol{\Psi}(x)\ , \boldsymbol{\Psi}''(x) = (\boldsymbol{B}_{\boldsymbol{T}}^*)^2\, \boldsymbol{\Psi}(x)\, , \dots\, , \boldsymbol{\Psi}^{(n)}(x) = (\boldsymbol{B}_{\boldsymbol{T}}^*)^n\, \boldsymbol{\Psi}(x),$$

where $\boldsymbol{B}_{\boldsymbol{T}\ (n+1)\times(n+1),}^*$ is the specified derivative's operational matrix, which is defined as follows:

$$\boldsymbol{B}_{\boldsymbol{T}}^* = (d_{i,j}) = \begin{cases} \dfrac{2i}{\mu_j}, & \text{for } j = i - k, \\ 0 & \text{otherwise}, \end{cases}$$

where $k = 1, 3, 5, \dots, n-1$ if $n$ is even, or $k = 1, 3, 5, \dots, n$ if $n$ is odd, $\mu_0 = 2$, and $\mu_k = 1$ for all $k \ge 1$.

For instance, if $n$ is even, the $\boldsymbol{B}_{\boldsymbol{T}}^*$ is written as follows:

$$\boldsymbol{B}_{\boldsymbol{T}}^{*}=\begin{pmatrix} 0 & 0 & 0 & 0 & 0 & \dots & 0 & 0 & 0 \\ 1 & 0 & 0 & 0 & 0 & \dots & 0 & 0 & 0 \\ 0 & 4 & 0 & 0 & 0 & \dots & 0 & 0 & 0 \\ 3 & 0 & 6 & 0 & 0 & \dots & 0 & 0 & 0 \\ 0 & 8 & 0 & 8 & 0 & \dots & 0 & 0 & 0 \\ 5 & 0 & 10 & 0 & 10 & \dots & 0 & 0 & 0 \\ \vdots & \vdots & \vdots & \vdots & \vdots & \ddots & 0 & 0 & 0 \\ n-1 & 0 & 2(n-1) & 0 & 2(n-1) & \dots & 2(n-1) & 0 & 0 \\ 0 & 2n & 0 & 2n & 0 & \dots & 0 & 2n & 0 \end{pmatrix}.$$

The matrix $\boldsymbol{B}_{\boldsymbol{T}}^{*}$ is also defined as follows if $n$ is odd:

$$\boldsymbol{B}_{\boldsymbol{T}}^{*}=\begin{pmatrix} 0 & 0 & 0 & 0 & \dots & 0 & 0 & 0 \\ 1 & 0 & 0 & 0 & \dots & 0 & 0 & 0 \\ 0 & 4 & 0 & 0 & \dots & 0 & 0 & 0 \\ 3 & 0 & 6 & 0 & \dots & 0 & 0 & 0 \\ 0 & 8 & 0 & 8 & \dots & 0 & 0 & 0 \\ \vdots & \vdots & \vdots & \vdots & \ddots & 0 & 0 & 0 \\ 0 & 2(n-1) & 0 & 2(n-1) & \dots & 2(n-1) & 0 & 0 \\ n & 0 & 2n & 0 & \dots & 0 & 2n & 0 \end{pmatrix}.$$

Consequently, the derivatives of the function $y(x)$ have the following form:

$$y^{(n)}(x)=\boldsymbol{A}^{T}\,(\boldsymbol{B}_{\boldsymbol{T}}^{*})^{n}\;\boldsymbol{\Psi}(x),\qquad \text{where, } n\geq 1. \tag{22}$$

### 3.3 The Bernoulli Polynomials and Their Operational Matrices

The definition of the Bernoulli polynomials $\boldsymbol{B}_{n}(x)$ of degree $n$ is as follows:

$$\boldsymbol{B}_{n}(x)=\sum_{i=0}^{n}\frac{n!\;\boldsymbol{b}_{i}}{i\,!\;(n-i)!\;2^{n-i}}\;(x+1)^{n-i}, \tag{23}$$

where $\boldsymbol{b}_{i}=\boldsymbol{B}_{i}(0)$ is called the Bernoulli number for each $i=0,1,\ldots$. These numbers are calculated by the following identity [62]:

$$\frac{x}{e^{x}-1}=\sum_{i=0}^{\infty}\boldsymbol{b}_{i}\frac{x^{i}}{i!},$$

The first few of the Bernoulli numbers are: $\boldsymbol{b}_{0}=1,\boldsymbol{b}_{1}=-\frac{1}{2},\boldsymbol{b}_{2}=\frac{1}{6},\boldsymbol{b}_{4}=-\frac{1}{30},\ldots$, and $\boldsymbol{b}_{2i+1}=0$ for $i\geq 1$.

We intend to approximate the solution $y(x)$ of the problem with the initial or boundary conditions in the form [44]:

$$y(x)=\sum_{k=0}^{n}a_{k}\,\boldsymbol{B}_{k}(x)=\;\boldsymbol{A}^{T}\,\boldsymbol{\Psi}(x), \tag{24}$$

where $\boldsymbol{\Psi}(x)=[\boldsymbol{B}_{0}(x),\boldsymbol{B}_{1}(x),\boldsymbol{B}_{2}(x),\ldots,,\boldsymbol{B}_{n}(x)]^{T}$ and $\boldsymbol{A}=[a_{0}\;a_{1}\;a_{2}\ldots a_{n}]^{T}$, such that $a_{k},k=0,\ldots,n,$ are the unknown Bernoulli coefficients, whose values will be identified later.

Furthermore, the derivatives of $\boldsymbol{\Psi}(x)$ can be expressed as:

$$\boldsymbol{\Psi}'(x)=\boldsymbol{B}_{\boldsymbol{\mathcal{B}}}^{*}\,\boldsymbol{\Psi}(x)\,,\boldsymbol{\Psi}''(x)=(\boldsymbol{B}_{\boldsymbol{\mathcal{B}}}^{*})^{2}\,\boldsymbol{\Psi}(x)\,,\ldots\,,\boldsymbol{\Psi}^{(n)}(x)=(\boldsymbol{B}_{\boldsymbol{\mathcal{B}}}^{*})^{n}\,\boldsymbol{\Psi}(x),$$

where $\boldsymbol{B}_{\boldsymbol{\mathcal{B}}\;(n+1)\times(n+1),}^{*}$ is the differentiation operational Bernoulli matrix, which is defined as follows [11]:

$$\boldsymbol{B}_{\mathcal{B}}^{*}=\begin{bmatrix}0&0&0&\dots&0&0\\1&0&0&\dots&0&0\\0&2&0&\cdots&0&0\\\vdots&\vdots&\vdots&\ddots&\vdots&\vdots\\0&0&0&\cdots&n&0\end{bmatrix}_{(n+1)\times(n+1)}$$

Then, the derivatives of the function $y(x)$ can be defined by:

$$y^{(n)}(x)=\boldsymbol{A}^{T}\,(\boldsymbol{B}_{\mathcal{B}}^{*})^{n}\,\,\boldsymbol{\Psi}(x),\qquad \text{where, } n\geq 1. \tag{25}$$

### 3.4 The Laguerre Polynomials and Their Operational Matrices

The Laguerre polynomials $\boldsymbol{L}_n(x)$ of degree $n$ are defined as follows [12]:

$$\boldsymbol{L}_n(x)=\sum_{k=0}^{n}(-1)^k\frac{n!}{(n-k)!\,(k!)^2}\,x^k\,,\qquad n\geq 0 \tag{26}$$

with $\boldsymbol{L}_n(0)=1$. Moreover, the first few Laguerre polynomials $\boldsymbol{L}_n(x)$ are as follows:

$$\boldsymbol{L}_0(x)=1,\;\;\boldsymbol{L}_1(x)=1-x,\;\;\boldsymbol{L}_2(x)=1-2\,x+\frac{x^2}{2},\;\;\boldsymbol{L}_3(x)=1-3\,x+\frac{3\,x^2}{2}-\frac{x^3}{6},\dots$$

The unknown function $y(x)$ can be approximated by the $(n+1)$-terms of the Laguerre polynomials as [17]:

$$y(x)=\sum_{k=0}^{n}a_k\,\boldsymbol{L}_k(x)=\boldsymbol{\Psi}(x)\,\boldsymbol{A}, \tag{27}$$

where, $\boldsymbol{\Psi}(x)=[\boldsymbol{L}_0(x),\boldsymbol{L}_1(x),\boldsymbol{L}_2(x),\dots,\boldsymbol{L}_n(x)]$ and $\boldsymbol{A}=[a_0\;a_1\;a_2\;\dots\;a_n]^T$, such that $a_k, k=0,\dots,n$, are the unknown Laguerre coefficients, whose values will be determined later.

In addition, the relation between the Laguerre polynomials $\boldsymbol{L}_n(x)$ and its integer order derivatives is defined by [17]:

$$\boldsymbol{\Psi}'(x)=\boldsymbol{\Psi}(x)\,\boldsymbol{B}_{\boldsymbol{L}}^{*}\,,\boldsymbol{\Psi}''(x)=\boldsymbol{\Psi}(x)\,(\boldsymbol{B}_{\boldsymbol{L}}^{*})^2,\dots\,,\boldsymbol{\Psi}^{(n)}(x)=\boldsymbol{\Psi}(x)\,(\boldsymbol{B}_{\boldsymbol{L}}^{*})^n,$$

where $\boldsymbol{B}_{\boldsymbol{L}\,(n+1)\times(n+1),}^{*}$ is the operational matrix of the provided derivative of the Laguerre polynomials, which is defined by [17]:

$$\boldsymbol{B}_{\boldsymbol{L}}^{*}=\begin{bmatrix}0&-1&-1&&-1\\0&0&-1&\cdots&-1\\0&0&0&&-1\\&\vdots&&\ddots&\vdots\\0&0&0&&-1\\0&0&0&\cdots&0\end{bmatrix}_{(n+1)\times(n+1)}.$$

Accordingly, the derivatives of the function $y(x)$ can be expressed by:

$$y^{(n)}(x)=\boldsymbol{\Psi}(x)\,(\boldsymbol{B}_{\boldsymbol{L}}^{*})^n\,\boldsymbol{A},\qquad \text{where, } n\geq 1. \tag{28}$$

## 4. The Implementation of the ECM and I-ECMs and Numerical Results

The proposed methods of the ECM and the I-ECMs will be applied in this section to find novel approximate solutions, and the numerical results will be presented for three nonlinear problems: the Darcy-Brinkman-Forchheimer equation, the Blasius equation, and the Falkner-Skan equation.

The I-ECMs are based on the base functions of diverse polynomials such as Chebyshev, Bernoulli, and Laguerre polynomials, introduced in Equations (20), (23), and (26), respectively, with relevant operational matrices. These polynomials are performed in two steps of the proposed method's procedures to improve the ECM's accuracy and reliability. First, describe the unknown function $y(x)$ and its derivatives; and second, calculate the inner product to solve the left and right sides of the matrix equation explained in Equation (18).

Furthermore, the initial or boundary conditions are substituted, as specified in Equations (15) and (16), and some entries of Equation (18) are modified. Therefore, we obtain $(n+1)$ nonlinear algebraic equations for the unknown coefficients$\boldsymbol{A}$. By solving this system numerically using Mathematica®12, we get the values for the unknown coefficients $a_0, a_1, a_2, \dots, a_n$ to obtain a novel approximate solution to the nonlinear initial and boundary value problems.

### 4.1 Solving the Darcy-Brinkman-Forchheimer Equation by the ECM and I-ECMs

The ECM and the I-ECMs techniques are used to solve the first problem presented in the Equation (1) with boundary conditions in Equation (2). More precisely, for the ECM technique, we transform the function $y(x)$ and its derivatives into matrices by substituting Equations (12) and (13) into Equations (1) and (2). Thus, we get the following result:

$$\boldsymbol{\Psi}(x)\ (\boldsymbol{B}^*)^2\ \boldsymbol{A} - s^2\ (\boldsymbol{\Psi}(x)\ \boldsymbol{A}) - Fs(\boldsymbol{\Psi}(x)\ \boldsymbol{A})^2 + \frac{1}{M} = 0,$$
$$\boldsymbol{\Psi}(0)\ \boldsymbol{B}^*\ \boldsymbol{A} = 0,\ \ \boldsymbol{\Psi}(1)\ \boldsymbol{A} = 0. \tag{29}$$

Then, the procedures have been applied, as shown in Equations (18) and (19), leading to:

$$\langle x^i,\ \ \boldsymbol{\Psi}(x)\ (\boldsymbol{B}^*)^2\ \boldsymbol{A} - s^2\ (\boldsymbol{\Psi}(x)\ \boldsymbol{A}) - Fs(\boldsymbol{\Psi}(x)\ \boldsymbol{A})^2\rangle = \langle x^i, -\frac{1}{M}\rangle,\ \ \forall\ 0 \le i \le n. \tag{30}$$

Substituting Equations (21) and (22) into Equations (1) and (2) for the I-ECMs based on the first kind of the Chebyshev polynomials, the following result is obtained:

$$\boldsymbol{A}^T\ (\boldsymbol{B}_{\boldsymbol{T}}^*)^2\ \ \boldsymbol{\Psi}(x) - s^2\ (\boldsymbol{A}^T\ \boldsymbol{\Psi}(x)) - Fs\big(\boldsymbol{A}^T\ \boldsymbol{\Psi}(x)\big)^2 + \frac{1}{M} = 0,$$
$$\boldsymbol{A}^T\ \boldsymbol{B}_{\boldsymbol{T}}^*\ \ \boldsymbol{\Psi}(0) = 0,\ \ \boldsymbol{A}^T\ \boldsymbol{\Psi}(1) = 0. \tag{31}$$

Additionally, the results of applying Equations (18) and (19) are as follows:

$$\langle \boldsymbol{T}_i(x), \boldsymbol{A}^T\ (\boldsymbol{B}_{\boldsymbol{T}}^*)^2\ \ \boldsymbol{\Psi}(x) - s^2\ (\boldsymbol{A}^T\ \boldsymbol{\Psi}(x)) - Fs\big(\boldsymbol{A}^T\ \boldsymbol{\Psi}(x)\big)^2\rangle = \langle \boldsymbol{T}_i(x), -\frac{1}{M}\rangle,\ \ \forall\ 0 \le i \le n. \tag{32}$$

Implementing the I-ECMs based on the Bernoulli polynomials by substituting Equations (24) and (25) into Equations (1) and (2), it follows:

$$\boldsymbol{A}^T\ (\boldsymbol{B}_{\boldsymbol{\mathcal{B}}}^*)^2\ \ \boldsymbol{\Psi}(x) - s^2\ (\boldsymbol{A}^T\ \boldsymbol{\Psi}(x)) - Fs\big(\boldsymbol{A}^T\ \boldsymbol{\Psi}(x)\big)^2 + \frac{1}{M} = 0,$$
$$\boldsymbol{A}^T\ \boldsymbol{B}_{\boldsymbol{\mathcal{B}}}^*\ \ \boldsymbol{\Psi}(0) = 0,\ \ \boldsymbol{A}^T\ \boldsymbol{\Psi}(1) = 0. \tag{33}$$

Using the technique described in Equations (18) and (19), the following equation will be given:

$$\langle \boldsymbol{B}_i(x), \boldsymbol{A}^T\ (\boldsymbol{B}_{\boldsymbol{\mathcal{B}}}^*)^2\ \ \boldsymbol{\Psi}(x) - s^2\ (\boldsymbol{A}^T\ \boldsymbol{\Psi}(x)) - Fs\big(\boldsymbol{A}^T\ \boldsymbol{\Psi}(x)\big)^2\rangle = \langle \boldsymbol{B}_i(x), -\frac{1}{M}\rangle,\ \ \forall\ 0 \le i \le n. \tag{34}$$

Moreover, applying the I-ECMs based on the Laguerre polynomials by substituting the Equations (27) and (28) into the Equations (1) and (2), we obtain:

$$\boldsymbol{\Psi}(x)\ (\boldsymbol{B}_{\boldsymbol{L}}^*)^2\ \boldsymbol{A} - s^2\ (\boldsymbol{\Psi}(x)\ \boldsymbol{A}) - Fs(\boldsymbol{\Psi}(x)\ \boldsymbol{A})^2 + \frac{1}{M} = 0,$$
$$\boldsymbol{\Psi}(0)\ \boldsymbol{B}_{\boldsymbol{L}}^*\ \boldsymbol{A} = 0,\ \ \boldsymbol{\Psi}(1)\ \boldsymbol{A} = 0. \tag{35}$$

Subsequently, the procedures as specified in Equations (18) and (19) have been utilized, as will be illustrated:

$$\langle \boldsymbol{L}_i(x), \boldsymbol{\Psi}(x)\ (\boldsymbol{B}_{\boldsymbol{L}}^*)^2\ \boldsymbol{A} - s^2\ (\boldsymbol{\Psi}(x)\ \boldsymbol{A}) - Fs(\boldsymbol{\Psi}(x)\ \boldsymbol{A})^2\rangle = \langle \boldsymbol{L}_i(x), -\frac{1}{M}\rangle,\ \ \forall\ 0 \le i \le n. \tag{36}$$

Additionally, the inner product for the left and right sides of Equations (30), (32), (34), and (36), respectively, is used to get the values of $\boldsymbol{A} = [a_0\ a_1\ a_2 \dots a_n]^T$ by solving the algebraic system of equations. Once the boundary conditions have been applied to Equations (29), (31), (33), and (35), respectively, the desired novel approximate solutions are obtained.

If the parameter values are $s = 1$, $F = 1$, and $M = 1$, as in [36], with $n = 10$, then the novel approximate solutions for the Darcy-Brinkman-Forchheimer equation will be:

By applying the ECM based on the standard polynomials:

$$y(x) \approx 0.323852 - 0.285634\,x^2 + 2.29576 \times 10^{-6} x^3 - 0.0392379\,x^4 + 0.0000786079\,x^5 + 0.000355229\,x^6 + 0.000352023\,x^7 + 0.0000516179\,x^8 + 0.00021914\,x^9 - 0.0000397161\,x^{10}.$$

Also, by implementing the I-ECMs based on the first kind of the Chebyshev polynomials, we obtain:

$$y(x) \approx 0.323852 - 0.285634\,x^2 + 8.64572 \times 10^{-7} x^3 - 0.039229\,x^4 + 0.0000472476\,x^5 + 0.000421857\,x^6 + 0.000264638\,x^7 + 0.000120859\,x^8 + 0.000188736\,x^9 - 0.0000340335\,x^{10}.$$

Moreover, by using the I-ECMs based on the Bernoulli polynomials, we achieve:

$$y(x) \approx 0.323852 - 0.285634\,x^2 + 8.72335 \times 10^{-7} x^3 - 0.039229\,x^4 + 0.0000475082\,x^5 + 0.000421236\,x^6 + 0.000265524\,x^7 + 0.000120109\,x^8 + 0.000189083\,x^9 - 0.0000341013\,x^{10}.$$

In addition, by utilizing the I-ECMs based on the Laguerre polynomials, we get:

$$y(x) \approx 0.323852 - 0.285634\,x^2 + 7.16738 \times 10^{-7} x^3 - 0.0392277\,x^4 + 0.0000418568\,x^5 + 0.000435078\,x^6 + 0.0002453\,x^7 + 0.000137559\,x^8 + 0.000180872\,x^9 - 0.0000324758\,x^{10}.$$

Furthermore, since the exact solution to the Darcy-Brinkman-Forchheimer equation is unknown, the $MER_n$ has been calculated to determine the accuracy and reliability of the novel approximate solution produced by the proposed approaches. The $MER_n$ is calculated by:

$$MER_n = \max_{0 \le x \le 1} \left| y''(x) - s^2 y(x) - Fsy^2(x) + \frac{1}{M} \right|.$$

Figure 2 presents the logarithmic plots for the $MER_n$ values obtained by the ECM based on the standard polynomials and by the I-ECMs based on the Chebyshev, Bernoulli, and Laguerre polynomials, which prove the efficiency and accuracy of these techniques by observation of the error values for $n =$ 2 to 10, as we found that the error decreases with increasing the values of $n$.

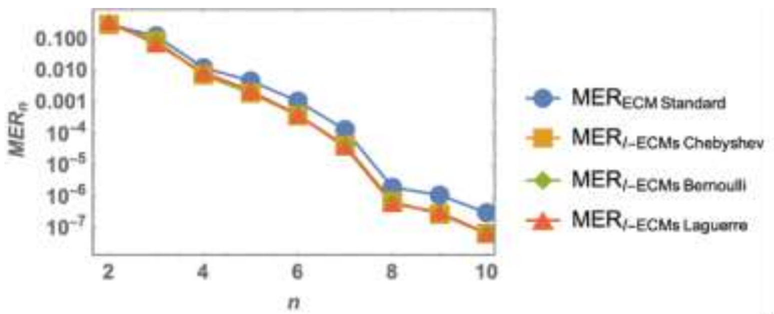


**Figure 2.** Logarithmic plots of $MER_n$ to the Darcy-Brinkman-Forchheimer equation.

Also, Figure 3 presents the comparison between the novel approximate solutions calculated by the proposed techniques for $n = 10, s = 1, F = 1$, and $M = 1$. It is evident that impressive agreements have been achieved for all the suggested methods.

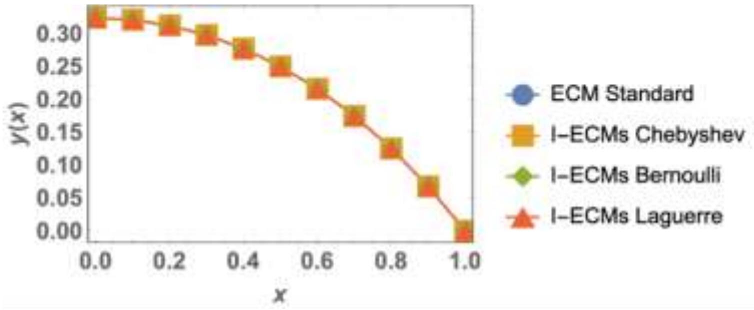


**Figure 3.** The comparison of the solutions to the Darcy-Brinkman-Forchheimer equation by proposed methods.

Moreover, the values of the $MER_n$ for the novel approximate solutions utilizing ECM and I-ECMs are also shown in Table 1 with $n = 10$ and parameters $s = M = 1$, versus the value of $F$, which offers the accuracy of these techniques. In addition, it can be observed that the I-ECMs based on the Chebyshev polynomial method provide slightly better accuracy with the lowest number of errors compared to other techniques.

**Table 1.** The comparison between the $MER_{10}$ when $s = M = 1$, and versus the value of $F$ for the Darcy-Brinkman-Forchheimer equation.

| *F* | ECM Standard | I-ECMs Chebyshev | I-ECMs Bernoulli | I-ECMs Laguerre |
|---|---|---|---|---|
| 2 | $1.27523 \times 10^{-6}$ | $2.75302 \times 10^{-7}$ | $2.7852 \times 10^{-7}$ | $2.77819 \times 10^{-7}$ |
| 4 | $5.33771 \times 10^{-6}$ | $1.14476 \times 10^{-6}$ | $1.15826 \times 10^{-6}$ | $1.17427 \times 10^{-6}$ |
| 6 | $0.0000118871$ | $2.52936 \times 10^{-6}$ | $2.5595 \times 10^{-6}$ | $2.65222 \times 10^{-6}$ |

## 4.2 Solving the Blasius Equation by the ECM and I-ECMs

The ECM and the I-ECMs techniques are utilized to solve the second problem shown in the Equations (3) and (5). More precisely, we substitute Equations (12) and (13) into Equations (3) and (5) for the technique ECM, converting the function $y(x)$ and its derivatives as matrices. Thus, we obtain the following result:

$$\boldsymbol{\Psi}(x)\ (\boldsymbol{B}^*)^3\ \boldsymbol{A} + \frac{1}{2}\ (\boldsymbol{\Psi}(x)\ \boldsymbol{A})(\boldsymbol{\Psi}(x)\ (\boldsymbol{B}^*)^2\ \boldsymbol{A}) = 0,$$
$$\boldsymbol{\Psi}(0)\ \boldsymbol{A} = 0,\ \ \boldsymbol{\Psi}(0)\ \boldsymbol{B}^*\ \boldsymbol{A} = 0,\ \ \ \boldsymbol{\Psi}(0)\ (\boldsymbol{B}^*)^2\ \boldsymbol{A} = \alpha. \tag{37}$$

Then, the processes have been applied, as shown in the Equations (18) and (19), so:

$$\langle x^i,\ \boldsymbol{\Psi}(x)\ (\boldsymbol{B}^*)^3\ \boldsymbol{A} + \frac{1}{2}\ (\boldsymbol{\Psi}(x)\ \boldsymbol{A})(\boldsymbol{\Psi}(x)\ (\boldsymbol{B}^*)^2\ \boldsymbol{A})\rangle = \langle x^i, 0\rangle,\ \ \forall\ 0 \le i \le n. \tag{38}$$

Substituting Equations (21) and (22) into Equations (3) and (5) for the I-ECMs based on the first kind of Chebyshev polynomials, it follows:

$$\boldsymbol{A}^T\ (\boldsymbol{B}_{\boldsymbol{T}}^*)^3\ \ \boldsymbol{\Psi}(x) + \frac{1}{2}\ (\boldsymbol{A}^T\ \boldsymbol{\Psi}(x))(\boldsymbol{A}^T\ (\boldsymbol{B}_{\boldsymbol{T}}^*)^2\ \ \boldsymbol{\Psi}(x)) = 0,$$
$$\boldsymbol{A}^T\ \boldsymbol{\Psi}(0) = 0,\ \ \boldsymbol{A}^T\ \boldsymbol{B}_{\boldsymbol{T}}^*\ \ \boldsymbol{\Psi}(0) = 0,\ \ \ \boldsymbol{A}^T\ (\boldsymbol{B}_{\boldsymbol{T}}^*)^2\ \ \boldsymbol{\Psi}(0) = \alpha. \tag{39}$$

And, the results of implementing Equations (18) and (19) are as follows:

$$\langle \boldsymbol{T}_i(x), \boldsymbol{A}^T\ (\boldsymbol{B}_{\boldsymbol{T}}^*)^3\ \ \boldsymbol{\Psi}(x) + \frac{1}{2}\ (\boldsymbol{A}^T\ \boldsymbol{\Psi}(x))(\boldsymbol{A}^T\ (\boldsymbol{B}_{\boldsymbol{T}}^*)^2\ \ \boldsymbol{\Psi}(x))\rangle = \langle \boldsymbol{T}_i(x), 0\rangle,\ \ \forall\ 0 \le i \le n. \tag{40}$$

Applying the I-ECMs based on the Bernoulli polynomials by substituting Equations (24) and (25) into Equations (3) and (5), the following is obtained:

$$\boldsymbol{A}^T\ (\boldsymbol{B}_{\mathcal{B}}^*)^3\ \boldsymbol{\Psi}(x)+\frac{1}{2}\ (\boldsymbol{A}^T\ \boldsymbol{\Psi}(x))(\boldsymbol{A}^T\ (\boldsymbol{B}_{\mathcal{B}}^*)^2\ \boldsymbol{\Psi}(x))=0,$$
$$\boldsymbol{A}^T\ \boldsymbol{\Psi}(0)=0,\ \ \boldsymbol{A}^T\ \boldsymbol{B}_{\mathcal{B}}^*\ \boldsymbol{\Psi}(0)=0,\ \ \ \boldsymbol{A}^T\ (\boldsymbol{B}_{\mathcal{B}}^*)^2\ \boldsymbol{\Psi}(0)=\alpha. \tag{41}$$

Using the procedures described in Equations (18) and (19), as a result, the following equation will be offered:

$$\langle \boldsymbol{B}_i(x), \boldsymbol{A}^T\ (\boldsymbol{B}_{\mathcal{B}}^*)^3\ \boldsymbol{\Psi}(x)+\frac{1}{2}\ (\boldsymbol{A}^T\ \boldsymbol{\Psi}(x))(\boldsymbol{A}^T\ (\boldsymbol{B}_{\mathcal{B}}^*)^2\ \boldsymbol{\Psi}(x))\rangle=\langle \boldsymbol{B}_i(x),0\rangle,\ \ \forall\ 0\le i\le n. \tag{42}$$

Moreover, implementing the I-ECMs based on the Laguerre polynomials by substituting Equations (27) and (28) into Equations (3) and (5), it follows that:

$$\boldsymbol{\Psi}(x)\ (\boldsymbol{B}_{\boldsymbol{L}}^*)^3\ \boldsymbol{A}+\frac{1}{2}\ (\boldsymbol{\Psi}(x)\ \boldsymbol{A})(\boldsymbol{\Psi}(x)\ (\boldsymbol{B}_{\boldsymbol{L}}^*)^2\ \boldsymbol{A})=0,$$
$$\boldsymbol{\Psi}(0)\ \boldsymbol{A}=0,\ \ \boldsymbol{\Psi}(0)\ \boldsymbol{B}_{\boldsymbol{L}}^*\ \boldsymbol{A}=0,\ \ \ \boldsymbol{\Psi}(0)\ (\boldsymbol{B}_{\boldsymbol{L}}^*)^2\ \boldsymbol{A}=\alpha. \tag{43}$$

Then, the processes have been utilized as given in Equations (18) and (19), which will be presented:

$$\langle \boldsymbol{L}_i(x), \boldsymbol{\Psi}(x)\ (\boldsymbol{B}_{\boldsymbol{L}}^*)^3\ \boldsymbol{A}+\frac{1}{2}\ (\boldsymbol{\Psi}(x)\ \boldsymbol{A})(\boldsymbol{\Psi}(x)\ (\boldsymbol{B}_{\boldsymbol{L}}^*)^2\ \boldsymbol{A})\rangle=\langle \boldsymbol{L}_i(x),0\rangle,\ \ \forall\ 0\le i\le n. \tag{44}$$

Furthermore, the inner product for the left and right sides of the Equations (38), (40), (42), and (44), respectively, is implemented to obtain the values of $\boldsymbol{A}=[a_0\ a_1\ a_2\ ...\ a_n]^T$by solving the algebraic system of equations. Then, the desired novel approximate solutions are achieved by applying the initial conditions to Equations (37), (39), (41), and (43), respectively.

In this problem, we consider the value of $\alpha=0.3320573$, as in [43] with $n=10$. The novel approximate polynomials for the Blasius equation are:

By using the ECM based on the standard polynomials:

$$\begin{aligned} y(x)\approx{}& 0.166029\,x^2+3.40035\times10^{-9}x^3-2.07849\times10^{-8}x^4-0.000459348\,x^5\\ &-1.85524\times10^{-7}x^6+2.93847\times10^{-7}x^7+2.1901\times10^{-6}x^8+2.05083\\ &\times10^{-7}x^9-8.02077\times10^{-8}x^{10}. \end{aligned}$$

Also, by applying the I-ECMs based on the first kind of the Chebyshev polynomials, we obtain:

$$\begin{aligned} y(x)\approx{}& 0.166029\,x^2+2.73849\times10^{-10}x^3-4.13564\times10^{-9}x^4-0.000459399\,x^5\\ &-8.68423\times10^{-8}x^6+1.75903\times10^{-7}x^7+2.2761\times10^{-6}x^8+1.70069\\ &\times10^{-7}x^9-7.41017\times10^{-8}x^{10}. \end{aligned}$$

Moreover, by implementing the I-ECMs based on the Bernoulli polynomials, we achieve:

$$\begin{aligned} y(x)\approx{}& 0.166029\,x^2+2.44299\times10^{-10}x^3-3.8326\times10^{-9}x^4-0.000459401\,x^5\\ &-8.36908\times10^{-8}x^6+1.71538\times10^{-7}x^7+2.27964\times10^{-6}x^8\\ &+1.68511\times10^{-7}x^9-7.38136\times10^{-8}x^{10}. \end{aligned}$$

In addition, by utilizing the I-ECMs based on the Laguerre polynomials, we get:

$$\begin{aligned} y(x)\approx{}& 0.166029\,x^2+1.27153\times10^{-10}x^3-2.35939\times10^{-9}x^4-0.000459408\,x^5\\ &-6.42605\times10^{-8}x^6+1.42272\times10^{-7}x^7+2.3051\times10^{-6}x^8+1.56588\\ &\times10^{-7}x^9-7.14836\times10^{-8}x^{10}. \end{aligned}$$

The exact solution to the Blasius equation is not available. Hence, the $MER_n$ has been calculated to demonstrate the accuracy of the novel approximate solutions obtained by the proposed techniques. The $MER_n$ is calculated by:

$$MER_n = \max_{0 \le x \le 1} \left| y'''(x) + \frac{1}{2} y(x)\, y''(x) \right|.$$

Figure 4 shows the logarithmic plots for the $MER_n$ values obtained by the ECM based on the standard polynomials and by the I-ECMs based on the Chebyshev, Bernoulli, and Laguerre polynomials, for $n = 3$ to 10, with a value of $\alpha = 0.3320573$, according to previous studies [43]. The accuracy and efficiency of these methods can be demonstrated by observing the error values for $n$, as we observed that the error decreases as the value of $n$ increases.

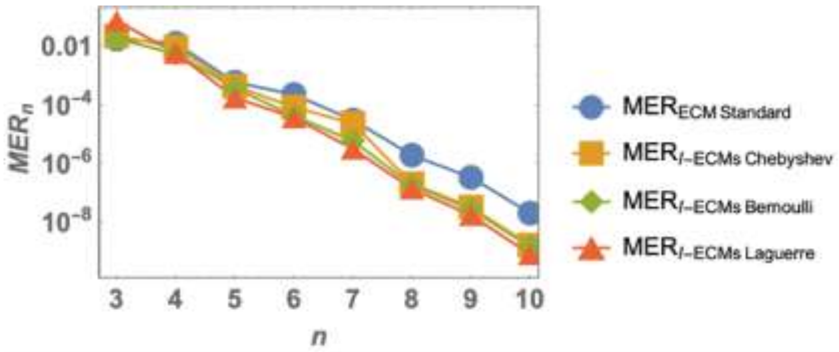


**Figure 4.** Logarithmic plots of $MER_n$ for the Blasius equation.

Figure 5 also illustrates the comparison between the novel approximate solutions calculated by the proposed techniques for $n = 10$ and $\alpha = 0.3320573$. The figure shows that all of the suggested methods have obtained good agreement.

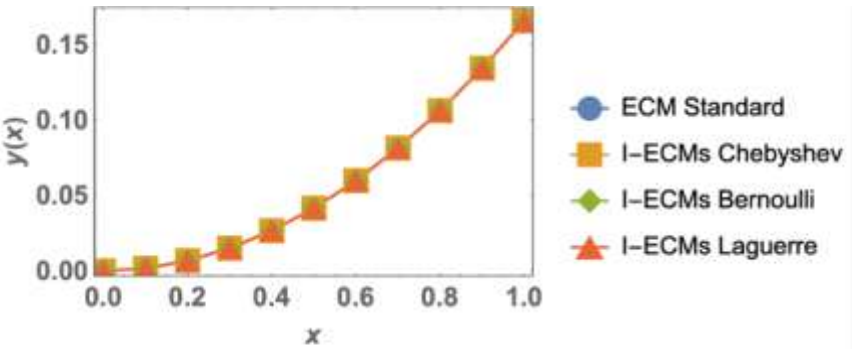


**Figure 5.** The comparison of the solutions for the Blasius equation.

Table 2 also presents the $MER_n$ values for the novel approximate solutions obtained with the ECM and the I-ECMs with $n = 10$, illustrating the efficacy of these methods. Furthermore, it can be seen that the I-ECMs based on the Laguerre polynomials technique give good accuracy with fewer errors compared to the other methods.

**Table 2.** The comparison between the $MER_{10}$ for the Blasius equation by proposed methods.

| $n$ | ECM Standard | I-ECMs Chebyshev | I-ECMs Bernoulli | I-ECMs Laguerre |
|---|---|---|---|---|
| 10 | $2.04021 \times 10^{-8}$ | $1.64309 \times 10^{-9}$ | $1.46579 \times 10^{-9}$ | $8.05404 \times 10^{-10}$ |

### 4.3 Solving the Falkner-Skan Equation by the ECM and I-ECMs

The procedures of the ECM and the I-ECMs techniques can be implemented to solve the third problem introduced in Equations (6) and (8). To be more specific, for the ECM technique, we transform the unknown function $y(x)$ with its derivatives as matrices by substituting the Equations (12) and (13) into Equations (6) and (8). Thus, we get the following result:

$$\boldsymbol{\Psi}(x)\ (\boldsymbol{B}^*)^3\ \boldsymbol{A} + (\boldsymbol{\Psi}(x)\ \boldsymbol{A})(\boldsymbol{\Psi}(x)\ (\boldsymbol{B}^*)^2\ \boldsymbol{A}) + \beta\ [\epsilon^2 - (\boldsymbol{\Psi}(x)\ \boldsymbol{B}^*\ \boldsymbol{A})^2] = 0,$$
$$\boldsymbol{\Psi}(0)\ \boldsymbol{A} = 0,\ \ \boldsymbol{\Psi}(0)\ \boldsymbol{B}^*\ \boldsymbol{A} = 1 - \epsilon,\ \ \boldsymbol{\Psi}(0)\ (\boldsymbol{B}^*)^2\ \boldsymbol{A} = -0.832666. \tag{45}$$

Then, the processes have been used as presented in the Equations (18) and (19), so:

$$\langle x^i, \boldsymbol{\Psi}(x)\ (\boldsymbol{B}^*)^3\ \boldsymbol{A} + (\boldsymbol{\Psi}(x)\ \boldsymbol{A})(\boldsymbol{\Psi}(x)\ (\boldsymbol{B}^*)^2\ \boldsymbol{A}) + \beta\ [-(\boldsymbol{\Psi}(x)\ \boldsymbol{B}^*\ \boldsymbol{A})^2]\ \rangle$$
$$= \langle x^i, -\beta\ \epsilon^2\rangle,\ \ \forall\ 0 \le i \le n. \tag{46}$$

Substituting Equations (21) and (22) into Equations (6) and (8) for the I-ECMs based on the first kind of the Chebyshev polynomials yields the following:

$$\boldsymbol{A}^T\ (\boldsymbol{B}_{\boldsymbol{T}}^*)^3\ \ \boldsymbol{\Psi}(x) + (\boldsymbol{A}^T\ \boldsymbol{\Psi}(x))(\boldsymbol{A}^T\ (\boldsymbol{B}_{\boldsymbol{T}}^*)^2\ \ \boldsymbol{\Psi}(x)) + \beta\ [\epsilon^2 - (\boldsymbol{A}^T\ \boldsymbol{B}_{\boldsymbol{T}}^*\ \ \boldsymbol{\Psi}(x))^2] = 0,$$
$$\boldsymbol{A}^T\ \boldsymbol{\Psi}(0) = 0,\ \ \boldsymbol{A}^T\ \boldsymbol{B}_{\boldsymbol{T}}^*\ \ \boldsymbol{\Psi}(0) = 1 - \epsilon,\ \ \boldsymbol{A}^T\ (\boldsymbol{B}_{\boldsymbol{T}}^*)^2\ \ \boldsymbol{\Psi}(0) = -0.832666. \tag{47}$$

And, by applying the processes shown in the Equations (18) and (19), the following results:

$$\langle \boldsymbol{T}_i(x),\ \boldsymbol{A}^T\ (\boldsymbol{B}_{\boldsymbol{T}}^*)^3\ \ \boldsymbol{\Psi}(x) + (\boldsymbol{A}^T\ \boldsymbol{\Psi}(x))(\boldsymbol{A}^T\ (\boldsymbol{B}_{\boldsymbol{T}}^*)^2\ \ \boldsymbol{\Psi}(x)) + \beta\ [-(\boldsymbol{A}^T\ \boldsymbol{B}_{\boldsymbol{T}}^*\ \ \boldsymbol{\Psi}(x))^2]\rangle$$
$$= \langle \boldsymbol{T}_i(x), -\beta\ \epsilon^2\rangle,\ \ \forall\ 0 \le i \le n. \tag{48}$$

Implementing the I-ECMs based on the Bernoulli polynomials by substituting Equations (24) and (25) into Equations (6) and (8), the following is achieved:

$$\boldsymbol{A}^T\ (\boldsymbol{B}_{\mathcal{B}}^*)^3\ \ \boldsymbol{\Psi}(x) + (\boldsymbol{A}^T\ \boldsymbol{\Psi}(x))(\boldsymbol{A}^T\ (\boldsymbol{B}_{\mathcal{B}}^*)^2\ \ \boldsymbol{\Psi}(x)) + \beta\ [\epsilon^2 - (\boldsymbol{A}^T\ \boldsymbol{B}_{\mathcal{B}}^*\ \ \boldsymbol{\Psi}(x))^2] = 0,$$
$$\boldsymbol{A}^T\ \boldsymbol{\Psi}(0) = 0,\ \ \boldsymbol{A}^T\ \boldsymbol{B}_{\mathcal{B}}^*\ \ \boldsymbol{\Psi}(0) = 1 - \epsilon,\ \ \boldsymbol{A}^T\ (\boldsymbol{B}_{\mathcal{B}}^*)^2\ \ \boldsymbol{\Psi}(0) = -0.832666. \tag{49}$$

Also, by using the techniques as specified in Equations (18) and (19), it follows that:

$$\langle \boldsymbol{B}_i(x),\ \boldsymbol{A}^T\ (\boldsymbol{B}_{\mathcal{B}}^*)^3\ \ \boldsymbol{\Psi}(x) + (\boldsymbol{A}^T\ \boldsymbol{\Psi}(x))(\boldsymbol{A}^T\ (\boldsymbol{B}_{\mathcal{B}}^*)^2\ \ \boldsymbol{\Psi}(x)) + \beta\ [-(\boldsymbol{A}^T\ \boldsymbol{B}_{\mathcal{B}}^*\ \ \boldsymbol{\Psi}(x))^2]\rangle$$
$$= \langle \boldsymbol{B}_i(x), -\beta\ \epsilon^2\rangle,\ \ \forall\ 0 \le i \le n. \tag{50}$$

Moreover, applying the I-ECMs based on the Laguerre polynomials by substituting Equations (27) and (28) into Equations (6) and (8), we get:

$$\boldsymbol{\Psi}(x)\ (\boldsymbol{B}_{\boldsymbol{L}}^*)^3\ \boldsymbol{A} + (\boldsymbol{\Psi}(x)\ \boldsymbol{A})(\boldsymbol{\Psi}(x)\ (\boldsymbol{B}_{\boldsymbol{L}}^*)^2\ \boldsymbol{A}) + \beta\ [\epsilon^2 - (\boldsymbol{\Psi}(x)\ \boldsymbol{B}_{\boldsymbol{L}}^*\ \boldsymbol{A})^2] = 0,$$
$$\boldsymbol{\Psi}(0)\ \boldsymbol{A} = 0,\ \ \boldsymbol{\Psi}(0)\ \boldsymbol{B}_{\boldsymbol{L}}^*\ \boldsymbol{A} = 1 - \epsilon,\ \ \boldsymbol{\Psi}(0)\ (\boldsymbol{B}_{\boldsymbol{L}}^*)^2\ \boldsymbol{A} = -0.832666. \tag{51}$$

Then, the processes have been utilized as provided in Equations (18) and (19), which will be shown:

$$\langle \boldsymbol{L}_i(x),\ \ \boldsymbol{\Psi}(x)\ (\boldsymbol{B}_{\boldsymbol{L}}^*)^3\ \boldsymbol{A} +\ (\boldsymbol{\Psi}(x)\ \boldsymbol{A})(\boldsymbol{\Psi}(x)\ (\boldsymbol{B}_{\boldsymbol{L}}^*)^2\ \boldsymbol{A}) +\ \beta\ [-(\boldsymbol{\Psi}(x)\ \ \boldsymbol{B}_{\boldsymbol{L}}^*\ \boldsymbol{A})^2]\rangle$$
$$= \langle \boldsymbol{L}_i(x), -\beta\ \epsilon^2\rangle,\ \ \forall\ 0 \le i \le n. \tag{52}$$

Furthermore, the values of $\boldsymbol{A} = [a_0\ a_1\ a_2\ ...\ a_n]^T$ are calculated by solving the algebraic system of equations obtained by the inner product for the left and right sides of Equations (46), (48), (50), and (52), respectively. Then, we utilize the initial conditions to Equations (45), (47), (49), and (51), respectively, the desired novel approximate solutions are obtained.

The novel approximate polynomials for the Falkner-Skan equation when the parameter values are as follows: $\epsilon = 0.1, \beta = 0.5$, as in [53], with $n$=8, will be:

By implementing the ECM based on the standard polynomials:

$$y(x) \approx 0.9\ x - 0.416333\ x^2 + 0.0666511\ x^3 + 0.0000592155\ x^4 - 0.00313186\ x^5$$
$$+ 0.000639976\ x^6 + 0.0000210854\ x^7 - 0.0000188788\ x^8.$$

Also, by applying the I-ECMs based on the first kind of the Chebyshev polynomials, we obtain:

$$y(x) \approx 0.9\,x - 0.416333\,x^2 + 0.0666646\,x^3 + 0.0000169313\,x^4 - 0.00305864\,x^5 + 0.00056836\,x^6 + 0.0000581686\,x^7 - 0.0000267944\,x^8.$$

In addition, by utilizing the I-ECMs based on the Bernoulli polynomials, we get:

$$y(x) \approx 0.9\,x - 0.416333\,x^2 + 0.0666648\,x^3 + 0.0000164756\,x^4 - 0.00305823\,x^5 + 0.000568589\,x^6 + 0.000057627\,x^7 - 0.0000265718\,x^8.$$

Moreover, by using the I-ECMs based on the Laguerre polynomials, we achieve:

$$y(x) \approx -8.72066 \times 10^{-14} + 0.9\,x - 0.416333\,x^2 + 0.0666602\,x^3 + 0.0000532904\,x^4 - 0.00316698\,x^5 + 0.00071942\,x^6 - 0.0000423225\,x^7 - 9.73011 \times 10^{-7} x^8.$$

Since there is no exact solution to the Falkner-Skan equation, the $MER_n$ is computed in order to verify the efficiency and accuracy of the novel approximate solutions found by the ECM and the I-ECMs. The $MER_n$ is calculated by:

$$MER_n = \max_{0 \le x \le 1} |y'''(x) + y(x)\,y''(x) + \beta\,[\epsilon^2 - (y'(x))^2]|.$$

Figure 6 exhibits the logarithmic plots for the $MER_n$ values obtained for the parameters $\epsilon = 0.1$, and $\beta = 0.5$, according to studies [53], by the ECM based on the standard polynomials and by the I-ECMs based on the Chebyshev, Bernoulli, and Laguerre polynomials, which demonstrate the accuracy and efficiency of these techniques by observing the error values for $n = 2$ to 8. We observe that when $n$ is increased, the error decreased.

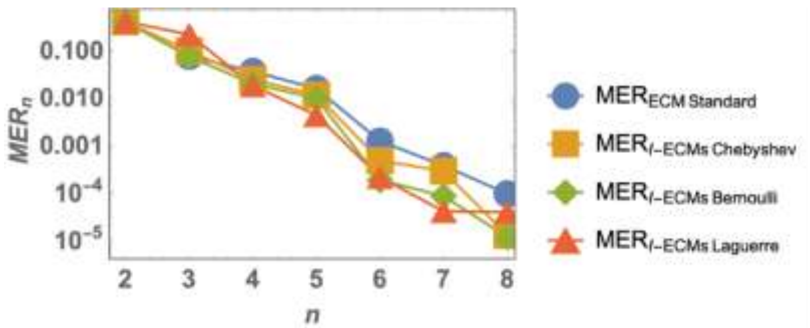


**Figure 6.** Logarithmic plots of $MER_n$ for the Falkner-Skan equation by proposed methods.

Also, Table 3 shows the $MER_n$ values for the novel approximate solutions achieved with the ECM and the I-ECMs with $n = 8$, explaining the accuracy of these methods. Moreover, the I-ECMs based on the Bernoulli polynomials method, offer slightly better accuracy and fewer errors than the other methods.

**Table 3.** The comparison between the $MER_8$ for the Falkner-Skan equation by proposed methods.

| $n$ | ECM Standard | I-ECMs Chebyshev | I-ECMs Bernoulli | I-ECMs Laguerre |
|---|---|---|---|---|
| 8 | 0.0000935074 | 0.0000123869 | 0.0000113839 | 0.0000385485 |

Moreover, Figure 7 shows the comparison between the novel approximate solutions calculated by the proposed techniques for $n = 8$, $\epsilon = 0.1$, and $\beta = 0.5$. The figure shows that all of the suggested approaches exhibited good agreement.

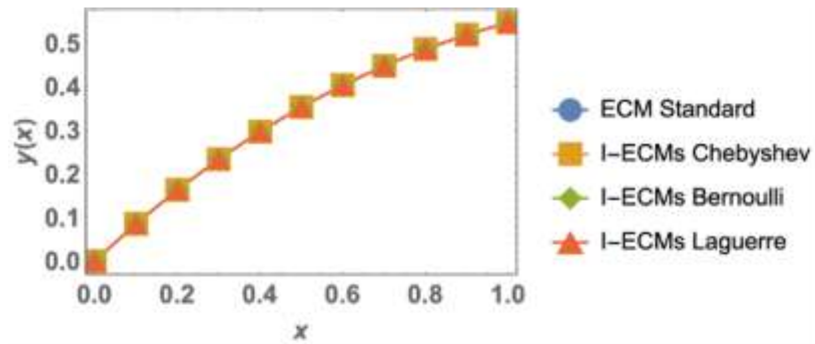


**Figure 7.** The comparison of the solutions to the Falkner-Skan equation by proposed methods.

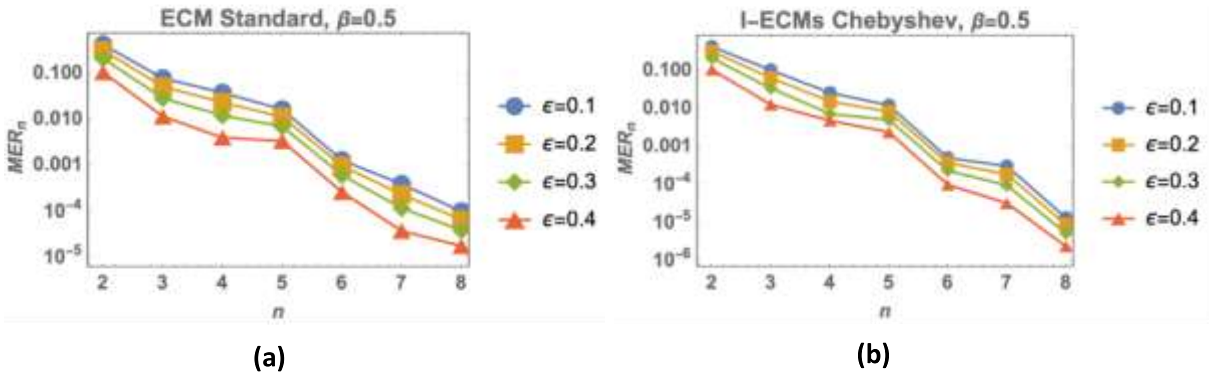


**Figure 8.** Logarithmic plots of $MER_n$ for the Falkner-Skan equation by (a) ECM based on the standard polynomials and (b) I-ECMs based on the Chebyshev polynomials.

In addition, Figures (8 and 9) explain the logarithmic plots of the $MER_n$ for the novel approximate solutions of the Falkner-Skan equation with $n = 2$ to 8, using the ECM and the I-ECMs when fixed the pressure gradient parameter $\beta = 0.5$, and increasing the values of the velocity ratio parameter as $\epsilon = 0.1, 0.2, 0.3,$ and $0.4,$ as chosen in [53]. In Figures (8 and 9), the errors decrease when the value of $\epsilon$ is increased.

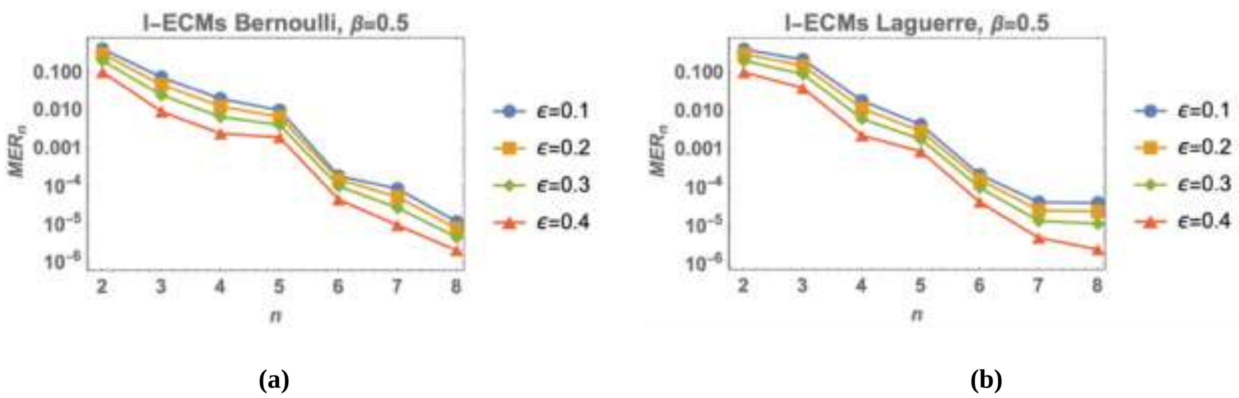


**Figure 9.** Logarithmic plots of $MER_n$ for the Falkner-Skan equation by (a) I-ECMs based on the Bernoulli polynomials and (b) I-ECMs based on the Laguerre polynomials.

Furthermore, Figures (10 and 11) illustrate the logarithmic plots of the $MER_n$ for the novel approximate solutions of the Falkner-Skan equation with $n = 2$ to 8, by using the ECM and the I-ECMs for different values of $\beta$ when fixed the parameter $\epsilon = 0.1$. In Figures (10 and 11), it is evident that the errors increase as the values of $\beta$ increase.

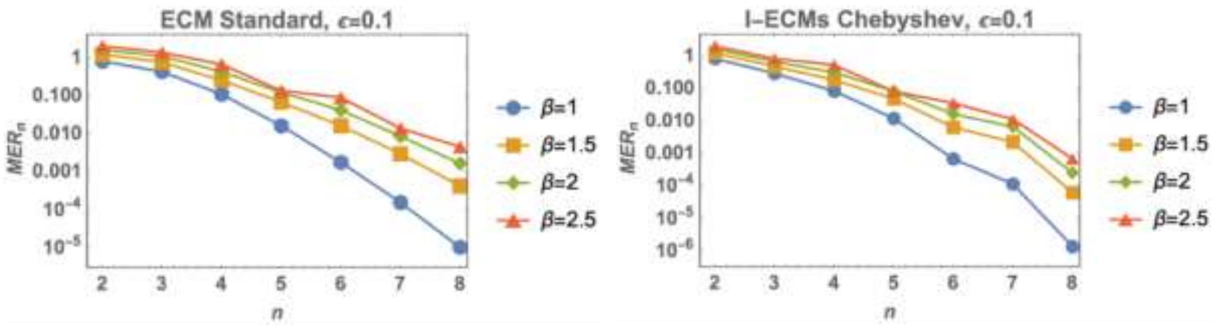


**(a)** **(b)**

**Figure 10.** Logarithmic plots of $MER_n$ for the Falkner-Skan equation by (a) ECM based on the standard polynomials and (b) I-ECMs based on the Chebyshev polynomials.

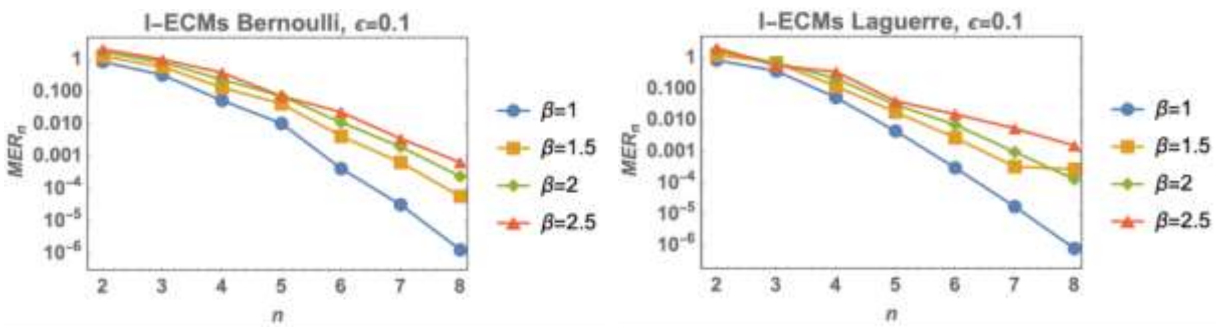


**(a)** **(b)**

**Figure 11.** Logarithmic plots of $MER_n$ for the Falkner-Skan equation by (a) I-ECMs based on the Bernoulli polynomials and (b) I-ECMs based on the Laguerre polynomials.

## 5. Conclusions

In this paper, the effective computational method based on standard polynomials and the novel effective computational methods based on the three different types of Chebyshev, Bernoulli, and Laguerre polynomials have been implemented to solve three nonlinear models involving initial and boundary value problems. Three models, which are well-known nonlinear problems: the Darcy-Brinkman-Forchheimer model, the Blasius model, and the Falkner-Skan model, have been presented and solved by using our suggested methods. The nonlinear problems are reduced to a nonlinear algebraic system of equations solved with Mathematica®12. The novel approximate solutions were obtained and proved accurate and reliable, even within a few polynomial orders. Moreover, the $MER_n$ for the proposed methods were calculated. The results show that the proposed approaches have higher accuracy and less error. It is also observed that the $MER_n$ results of the proposed methods I-ECMs decrease vastly compared to the ECM. Therefore, the proposed novel methods I-ECMs have better accuracy than the ECM. The main conclusion from the results is that the Chebyshev polynomials-based I-ECMs have slightly better accuracy than the other methods for solving the Darcy-Brinkman-Forchheimer equation. Moreover, the I-ECMs based on the Laguerre polynomials are more accurate than the other methods in solving the Blasius equation. In addition, the I-ECMs based on the Bernoulli polynomials are slightly more accurate than the other methods in solving the Falkner-Skan equation.

## References


1. Hermann, M.; Saravi, M. Nonlinear ordinary differential equations: Analytical approximation and numerical methods. *Springer India*, **2016**.
2. Kounadis, A. N. An efficient and simple approximate technique for solving nonlinear initial and boundary-value problems. *Computational Mechanics*, **1992**, *9(3)*, 221-231.
3. Talib, I.; Tunc, C.; Noor, Z. A. New operational matrices of orthogonal Legendre polynomials and their operational. *Journal of Taibah University for Science*, **2019**, *13*(*1*), 377-389.
4. AL-Jawary, M. A.; Salih, O. M. Reliable iterative methods for 1D Swift–Hohenberg equation. *Arab Journal of Basic and Applied Sciences*, **2020**, *27*(*1*), 56-66.
5. Umesh; Kumar, M. Numerical solution of singular boundary value problems using advanced Adomian decomposition method. *Engineering with Computers*, **2021**, *37*(*4)*, 2853-2863.
6. Harir, A.; Melliani, S.; El Harfi, H.; Chadli, L. S. Variational iteration method and differential transformation method for solving the SEIR epidemic model. *International Journal of Differential Equations*, **2020**, *2020*, 1-7.
7. Gohar, M.; Li, C.; Li, Z. Finite difference methods for Caputo–Hadamard fractional differential equations. *Mediterranean Journal of Mathematics*, **2020**, *17*(*6)*, 1-26.
8. Roul, P.; Thula, K. A new high-order numerical method for solving singular two-point boundary value problems. *Journal of Computational and Applied Mathematics*, **2018**, *343*, 556-574.
9. Ibraheem, K. I.; Mahmmood, H. S. Algorithm for solving fractional partial differential equations using homotopy analysis method with Pade approximation. *International Journal of Electrical and Computer Engineering*, **2022**, *12*(*3)*, 3335-3342.
10. Sharma, B.; Kumar, S.; Paswan, M. K.; Mahato, D. Chebyshev operational matrix method for Lane-Emden problem. *Nonlinear Engineering*, **2019**, *8*(*1*), 1-9.
11. Singh, S.; Patel, V. K.; Singh, V. K.; Tohidi, E. Application of Bernoulli matrix method for solving two-dimensional hyperbolic telegraph equations with Dirichlet boundary conditions. *Computers and Mathematics with Applications*, **2018**, *75*(*7*), 2280-2294.
12. Bhrawy, A. H.; Taha, T. M. An operational matrix of fractional integration of the Laguerre polynomials and its application on a semi-infinite interval. *Mathematical Sciences*, **2012**, *6*(*1*), 1-7.
13. AL-Jawary, M. A.; Abdul Nabi, A. J. Three iterative methods for solving Jeffery-Hamel flow problem. *Kuwait Journal of Science*, **2020**, *47*(*1*), 1-13.
14. Agom, E. U.; Ogunfiditimi, F. O.; Bassey, E. V. Homotopy perturbation and Adomian decomposition methods on 12th-order boundary value problems. *Advances in Mathematics: Scientific Journal*, **2020**, *9*(*12*), 10671-10683.

**15.** Singh, R. A modified homotopy perturbation method for nonlinear singular Lane–Emden equations arising in various physical models. *International Journal of Applied and Computational Mathematics*, **2019**, *5*(*3*), 1-15.

**16.** Ibraheem, G. H.; AL-Jawary, M. A. The operational matrix of Legendre polynomials for solving nonlinear thin film flow problems. *Alexandria Engineering Journal*, **2020**, *59*(*5*), 4027-4033.

**17.** Gürbüz, B.; Sezer, M. Modified operational matrix method for second-order nonlinear ordinary differential equations with quadratic and cubic terms. *An International Journal of Optimization and Control: Theories & Applications*, **2020**, *10*(*2*), 218-225.

**18.** Al-Humedi, H. O.; Al-Saadawi, F. A. The numerical technique based on shifted Jacobi-Gauss-Lobatto polynomials for solving two dimensional multi-space fractional Bioheat equations. *Baghdad Science Journal*, **2020**, *17*(*4*), 1271-1282.

**19.** Al-A'asam, J. A. Deriving the composite Simpson rule by using Bernstein polynomials for solving Volterra integral equations. *Baghdad Science Journal*, **2014**, *11*(*3*), 1274-1282.

**20.** AL-Jawary, M. A.; Ibraheem, G. H. Two meshless methods for solving nonlinear ordinary differential equations in engineering and applied sciences. *Nonlinear Engineering*, **2020**, *9*(*1*), 244-255.

**21.** Hasan, P. M.; Sulaiman, N. A. Convergence analysis for the homotopy perturbation method for a linear system of mixed Volterra-Fredholm integral equations. *Baghdad Science Journal*, **2020**, *17*(*3* (Suppl.)), 1010-1018.

**22.** Ateeah, A. K. Approximate solution for fuzzy differential algebraic equations of fractional order using Adomian decomposition method. *Ibn AL-Haitham Journal for Pure and Applied Science*, **2017**, *30*(*2*), 202-213.

**23.** Abed, S. M.; AL-Jawary, M. A. Efficient iterative methods for solving the SIR epidemic model. *Iraqi Journal of Science*, **2021**, *62*(*2*), 613-622.

**24.** Sparis, P. D.; Mouroutsos, S. G. The operational matrix of differentiation for orthogonal polynomial series. *International Journal of Control*, **1986**, *44*(*1*), 1-15.

**25.** Yousefi, S. A.; Behroozifar, M. Operational matrices of Bernstein polynomials and their applications. *International Journal of Systems Science*, **2010**, *41*(*6*), 709-716.

**26.** Öztürk, Y. Numerical solution of systems of differential equations using operational matrix method with Chebyshev polynomials. *Journal of Taibah University for Science*, **2018**, *12*(*2*), 155-162.

**27.** Bazm, S.; Hosseini, A. Bernoulli operational matrix method for the numerical solution of nonlinear two-dimensional Volterra–Fredholm integral equations of Hammerstein type. *Computational and Applied Mathematics*, **2020**, *39*(*2*), 1-20.

**28.** Abdelkawy, M. A.; Taha, T. M. An operational matrix of fractional derivatives of Laguerre polynomials. *Walailak Journal of Science and Technology*, **2014**, *11*(*12*), 1041-1055.

**29.** Turkyilmazoglu, M. Effective computation of exact and analytic approximate solutions to singular nonlinear equations of Lane–Emden–Fowler type. *Applied Mathematical Modelling*, **2013**, *37*(*14-15*), 7539-7548.

**30.** Turkyilmazoglu, M. An effective approach for numerical solutions of high-order Fredholm integro-differential equations. *Applied Mathematics and Computation*, **2014**, *227*(*15*), 384-398.

**31.** Turkyilmazoglu, M. High-order nonlinear Volterra–Fredholm-Hammerstein integro-differential equations and their effective computation. *Applied Mathematics and Computation*, **2014**, *247*, 410-416.

**32.** Turkyilmazoglu, M. Effective computation of solutions for nonlinear heat transfer problems in fins. *Journal of Heat Transfer*, **2014**, *136*(*9*), 091901.

**33.** Turkyilmazoglu, M. Solution of initial and boundary value problems by an effective accurate method. *International Journal of Computational Methods*, **2017**, *14*(*06*), 1750069.

**34.** Shaban, M.; Kazem, S.; Rad, J. A. A modification of the homotopy analysis method based on Chebyshev operational matrices. *Mathematical and Computer Modelling*, **2013**, *57*(*5-6*), 1227-1239.

**35.** Motsa, S. S.; Sibanda, P.; Shateyi, S. A new spectral-homotopy analysis method for solving a nonlinear second order BVP. *Communications in Nonlinear Science and Numerical Simulation*, **2010**, *15*(*9*), 2293-2302.

**36.** Manafian, J. An optimal Galerkin-homotopy asymptotic method applied to the nonlinear second-order BVPs. *Proceedings of the Institute of Mathematics and Mechanics*, **2021**, *47*(*1*), 156-182.

**37.** Waqas, M.; Gulzar, M. M.; Dogonchi, A. S.; Javed, M. A.; Khan, W. A. Darcy–Forchheimer stratified flow of viscoelastic nanofluid subjected to convective conditions. *Applied Nanoscience*, **2019**, *9*(*8)*, 2031-2037.

**38.** Awartani, M. M.; Hamdan, M. H. Fully developed flow through a porous channel bounded by flat plates. *Applied mathematics and computation*, **2005**, *169*(*2)*, 749-757.

**39.** Adewumi, A. O.; Akindeinde, S. O.; Aderogba, A. A.; Ogundare, B. S. A hybrid collocation method for solving highly nonlinear boundary value problems. *Heliyon*, **2020**, *6*(*3*), 1-10.

**40.** Abbasbandy, S.; Shivanian, E.; Hashim, I. Exact analytical solution of forced convection in a porous-saturated duct. *Communications in Nonlinear Science and Numerical Simulation*, **2011**, *16*(*10*), 3981-3989.

**41.** El-Gamel, M.; El-Shenawy, A. A numerical solution of Blasius equation on a semi-infinity flat plate. *SeMA Journal*, **2018**, *75*(*3*), 475-484.

**42.** Khataybeh, S. N.; Hashim, I.; Alshbool, M. Solving directly third-order ODEs using operational matrices of Bernstein polynomials method with applications to fluid flow equations. *Journal of King Saud University-Science*, **2019**, *31*(*4*), 822-826.

**43.** Liao, S. An optimal homotopy-analysis approach for strongly nonlinear differential equations. *Communications in Nonlinear Science and Numerical Simulation*, **2010**, *15*(*8*), 2003-2016.

**44.** Rani, D.; Mishra, V. Numerical inverse Laplace transform based on Bernoulli polynomials operational matrix for solving nonlinear differential equations. *Results in Physics*, **2020**, *16*, 102836.

**45.** Yao, B.; Chen, J. A new analytical solution branch for the Blasius equation with a shrinking sheet. *Applied Mathematics and Computation*, **2009**, *215*(*3*), 1146-1153.

**46.** Marinca, V.; Herişanu, N. The optimal homotopy asymptotic method for solving Blasius equation. *Applied Mathematics and Computation*, **2014**, *231*, 134-139.

**47.** Wazwaz, A. M. The variational iteration method for solving two forms of Blasius equation on a half-infinite domain. *Applied Mathematics and Computation*, **2007**, *188*(*1)*, 485-491.

**48.** Abbasbandy, S. A numerical solution of Blasius equation by Adomian’s decomposition method and comparison with homotopy perturbation method. *Chaos, Solitons & Fractals*, **2007**, *31*(*1*), 257-260.

**49.** Parand, K.; Taghavi, A. Rational scaled generalized Laguerre function collocation method for solving the Blasius equation. *Journal of Computational and Applied Mathematics*, **2009**, *233*(*4*), 980-989.

**50.** Abbasbandy, S.; Hajishafieiha, J. Numerical solution to the Falkner-Skan equation: a novel numerical approach through the new rational a-polynomials. *Applied Mathematics and Mechanics*, **2021**, *42*(*10*), 1449-1460.

**51.** Falkner, V. M.; Skan, S. W. Solutions of the boundary-layer equations. *The London, Edinburgh, and Dublin Philosophical Magazine and Journal of Science*, **1931**, *12*(*80*), 865-896.

**52.** Bakodah, H. O.; Ebaid, A.; Wazwaz, A. M. Analytical and numerical treatment of Falkner-Skan equation via a transformation and Adomian’s method. *Romanian Reports in Physics*, **2018**, *70*(*2*), 1-17.

**53.** AL-Jawary, M. A.; Adwan, M. I. Reliable iterative methods for solving the Falkner-Skan equation. *Gazi University Journal of Science*, **2020**, *33*(*1*), 168-186.

**54.** Moallemi, N.; Shafieenejad, I.; Hashemi, S. F.; Fata, A. Approximate explicit solution of Falkner-Skan equation by homotopy perturbation method. *Research Journal of Applied Sciences, Engineering and Technology*, **2012**, *4*(*17*), 2893-2897.

**55.** Abbasbandy, S.; Hayat, T. Solution of the MHD Falkner-Skan flow by homotopy analysis method. *Communications in Nonlinear Science and Numerical Simulation*, **2009**, *14*(*9-10*), 3591-3598.

**56.** Elgazery, N. S. Numerical solution for the Falkner-Skan equation. *Chaos, Solitons & Fractals*, **2008**, *35*(*4*), 738-746.

**57.** Kuo, B. L. Application of the differential transformation method to the solutions of Falkner-Skan wedge flow. *Acta Mechanica*, **2003**, *164*(*3*), 161-174.

**58.** Temimi, H.; Ben-Romdhane, M. Numerical solution of Falkner-Skan equation by iterative transformation method. *Mathematical Modelling and Analysis*, **2018**, *23*(*1*), 139-151.

**59.** Guo, B. Y.; Shen, J.; Wang, Z. Q. A rational approximation and its applications to differential equations on the half line. *Journal of scientific computing*, **2000**, *15*(*2*), 117-147.

**60.** Kajani, M. T.; Maleki, M.; Allame, M. A numerical solution of Falkner-Skan equation via a shifted Chebyshev collocation method. *AIP Conference Proceedings*, **2014**, *1629*(*1*), 381-386.

**61.** Calvert, V.; Razzaghi, M. Solutions of the Blasius and MHD Falkner-Skan boundary-layer equations by modified rational Bernoulli functions. *International Journal of Numerical Methods for Heat & Fluid Flow*, **2017**, *27*(*8*), 1687-1705.

**62.** Azodi, H. D.; Yaghouti, M. R. Bernoulli polynomials collocation for weakly singular Volterra integro-differential equations of fractional order. *Filomat*, **2018**, *32*(*10*), 3623-3635.